Electronic Supplementary Information

An activated near-infrared mitochondrion-targetable fluorescent probe for rapid detecting of NADH

Yaxin Sun[a], Yanyun Mao[b], Tianwen Bai[b], Tianqing Ye[b], Yanfei Lin[b], Fang Wang[a], Lei Li[b], Longhua Guo[b],*, Haiying Liu[c],* and Jianbo Wang[b],*

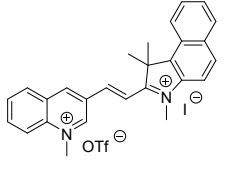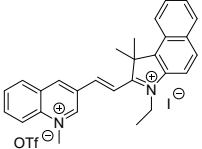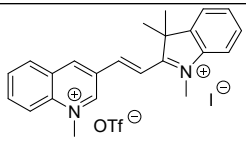[a]College of Pharmacy, Zhejiang University of Technology, Hangzhou, 310014, China
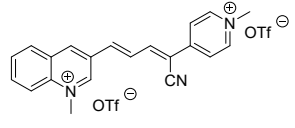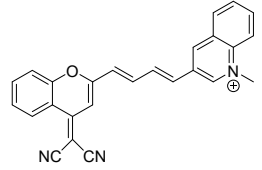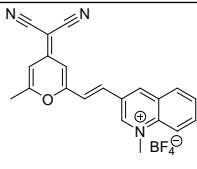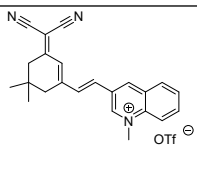
[b]Jiaxing Key Laboratory of Molecular Recognition and Sensing, College of Biological, Chemical Sciences and Engineering, Jiaxing University, Jiaxing 314001, China. E-mail: guolh@zjxu.edu.cn; wjb4207@mail.ustc.edu.cn.
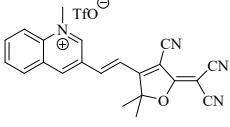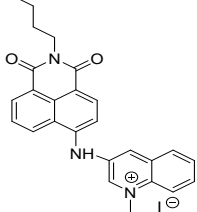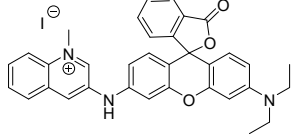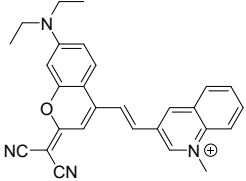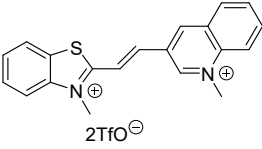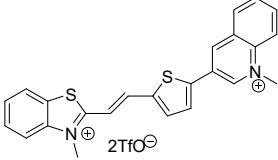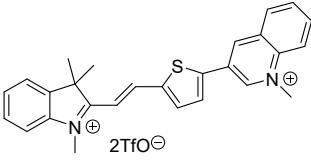
[c]Department of Chemistry, Michigan Technological University, Houghton, MI 49931, USA. E-mail: hyliu@mtu.edu

Table of Contents

Table 1 Summary of near-infrared fluorescent probes for specific detection of NADH.

Name of probe	Structures of probe	Limit of detection	λ_{em} (nm)	Response time	Application	references
Mito-FCC		0.26 μM	580	10 min	Imaging in cells	[1]
NAFP4		3.66 nM	584	3 min	Imaging in cells	[2]
Indicator1		0.1 μM	561	5 min	Imaging in cells and tumor spheroid model	[3]
NADH-R		12 nM	657	25 min	Imaging in cells and brain tissues	[4]
Probe 3Q-2		--	670	30 min	Imaging in cells	[5]
DPMQL1		0.36 nM	624	60 min	/	[6]
DCI-MQ		12 nM	680 (NIR)	15 min	Imaging in cells and tumor mice	[7]

3

TCF-MQ		6 nM	610	40 min	Imaging in cells and tumor mice	[8]
MQN		1.075 μM 1.114 μM	460 550	50 min	Imaging in cells and tumor spheroid	[9]
MQR		---	548	240 min	Imaging in cells	[10]
Probe 1		0.1 μM	640	80 min	Imaging in cells	[11]
Probe A		0.085 μM	572	6 min	Imaging in cells and drosophila melanogaster (Fruit flies)	[12]
Probe A		0.151 μM	748 (NIR)	50 min	Imaging in cells and drosophila melanogaster (Fruit flies)	[13]
Probe A		0.18 μM	742 (NIR)	60 min	Cells Drosophila melanogaster (Fruit flies)	[14]

KC8		---	750 (NIR)	66 min	Imaging in cells and tumor spheroid	[15]
Rh-QL		9.7 μM	750 (NIR)	About 70 min	Imaging in cells	[16]
QB		**43 nM**	**686 (NIR)**	**6 min**	**Imaging in cells; different types of cells and diabetes model cells**	**This work**

Experimental section

Materials and Instrumentation

Chemical agents were employed without purification unless otherwise indicated. Organic solvents were subjected to distillation before usage, and "pure water" refers to double-distilled water. UV-Vis absorption and fluorescence emission spectra were obtained using the Agilent Cary 5000 UV–vis spectrometer and the Edinburgh FS5 Spectrofluorometer, respectively. Mass spectra were acquired using the Thermo Scientific Q Exactive Orbitrap mass spectrometer. 1H and 13C NMR spectral data were recorded utilizing the Bruker AV-400M spectrometer.

Synthesis of probe QB.
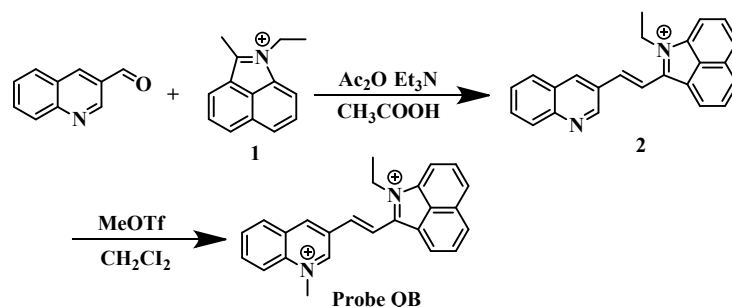
Scheme **S1** Synthetic route to prepare probe **QB**

In a synthetic procedure, 1-methylquinoline aldehyde (200 mg, 1.27 mmol) and compound 1 (1-ethyl-2-methylbenzo[cd]indol-1-ium iodide, 200 mg, 1.27 mmol) were dissolved in 6 mL of acetic acid (CH$_3$COOH). To this solution, 0.6 mL each of triethylamine and acetic anhydride were carefully added. The resulting mixture was stirred at 60°C for 1 hour. After cooling to room temperature, 10 mL of anhydrous ether was cautiously added dropwise. The precipitated solid was subsequently filtered, washed with ethyl acetate, and dried to yield compound 2 (320 mg, 91% yield). The characterization of compound **2** was carried out using ^{1}H NMR spectroscopy (400 MHz, d$_6$-DMSO), revealing characteristic peaks at δ: 9.69 (s, 1H), 9.45 (s, 1H), 9.21 (s, 1H), 8.98 (d, J = 15.6 Hz, 1H), 8.80 (s, 1H), 8.51 (s, 1H), 8.45 (s, 1H), 8.33 (d, J = 15.6 Hz, 1H), 8.23 (s, 1H), 8.12 (d, J = 8 Hz, 2H), 8.02 (s, 1H), 7.92 (s, 1H), 7.75 (t, J = 7.2 Hz, 1H), 4.97 (d, J = 4.8 Hz, 2H), 1.59 (t, J = 6.8 Hz, 3H). Additionally, mass spectrometry (ESI) yielded a calculated mass for C$_{24}$H$_{19}$N$_2^+$ [M]$^+$ of 335.1543, which closely matched the found mass of 335.1538.

Compound **2** (120 mg, 0.26 mmol) was combined with methyl trifluoro-methanesulfonate (127 mg, 0.78 mmol) in a solution of 10 mL of CH$_2$Cl$_2$. The resulting mixture underwent stirring for 48 hours at 25°C. Following the completion of the reaction, the solvent was eliminated via suction filtration. The resultant solid was subsequently washed successively with petroleum ether, ether, and dichloromethane. This meticulous process culminated in the isolation of the desired probe **QB** as a product (150 mg, 92% yield). Characterization by ^{1}H

NMR (400 MHz, CD3OD) revealed peaks at δ: 10.12 (s, 1H), 9.85 (s, 1H), 9.34 (d, J = 6.8 Hz, 1H), 8.93-8.89 (m, 1H), 8.79 (d, J = 8.8 Hz, 1H), 8.61-8.55 (m, 2H), 8.51-8.46 (m, 2H), 8.41-8.38 (m, 2H), 8.25 (t, J = 7.2 Hz, 1H), 8.16 (t, J = 6.8 Hz, 1H), 8.05 (t, J = 8 Hz, 1H), 5.01 (t, J = 7.2 Hz, 2H), 4.84 (s, 3H), 1.76 (t, J = 7.2 Hz, 3H). ^{13}C NMR (100 MHz, CD_3OD) exhibited peaks at δ: 161.3, 146.6, 146.0, 145.6, 145.3, 138.9, 138.6, 138.5, 137.3, 136.2, 132.3, 132.2, 130.1, 129.3, 129.2, 128.8, 127.3, 123.3, 122.0, 121.2, 121.1, 118.8, 45.4, 42.4, 15.0. MS (ESI) analysis displayed calculated values for [M]+ at 175.0886, with the actual found value at 175.0882 for $C_{25}H_{22}N_{22}^{+}$.

Preparation of sample testing solutions

The probe **QB** was initially dissolved in DMSO to create a 2.5 mM stock solution. Similarly, NADH (2.5 mM) and various amino acids (12.5 mM) were dissolved directly in deionized water to prepare their respective stock solutions. For experimental purposes, a pH 7.4 aqueous solution of PBS with a concentration of 20 mM was utilized. All chemicals utilized in the experiment were of analytical grade. To create a testing sample of the probe **QB** at a concentration of 10 μM, 10 μL of the stock solution was mixed with 2.5 mL of the aforementioned PBS solution. Subsequently, various analytes were added to deionized water at a concentration of 100 μM, and both absorption and fluorescence spectra were recorded for further analysis. The fluorescence quantum yields of the probe and its responsive reaction products were calculated using CS-2 as a reference standard (Φ_{st}=0.41 in EtOH)[17].

Intracellular Imaging.

HeLa, A549, HepG2, and 3T3 cell lines were cultured in DMEM supplemented with 1% penicillin-streptomycin and 10% fetal bovine serum (FBS), maintaining them at 37°C in a 5% CO_2 humidified environment. Initially, cells were seeded onto confocal dishes at a density of 5 x 10^4 cells per dish and allowed to adhere for 24 hours. Subsequently, a probe solution in DMSO was introduced, and the cells were cultured. We conducted a series of experiments to evaluate the imaging capabilities of the probe **QB** upon interaction with NADH. In the exogenous experiment, cells were pre-treated with 10 μM of the probe for 30 minutes, followed by exposure to varying concentrations of NADH for an additional 30 minutes. Conversely, in the endogenous experiment, glucose was utilized to stimulate NADH production within the cells, while pyruvate served to inhibit its production via lactate dehydrogenase. As such, cells were exposed to 20 mM glucose or 5 mM pyruvate for 30 minutes. To discern the probe **QB**'s ability to differentiate between cancerous and normal cells, we observed fluorescence intensity alterations in various cancers and normal cells post a 30-minute treatment with 10 μM of the probe.

Furthermore, the probe **QB** was employed to monitor NADH fluctuations in a type II diabetes cell model. Specifically, A549 cells were pre-treated with varying concentrations of DEX (10, 20 μM) for 24 hours to

induce insulin resistance. Following this, they were exposed to 10 µM of the probe for an additional 30 minutes. For a deeper insight into the fluorescence imaging capabilities of the probe after treatment of type II diabetic cells, cells were initially treated with DEX for 24 hours. Subsequent exposure to 50 µM metformin for an additional 24 hours was followed by a 30-minute incubation with the probe (10 µM).

Finally, the probe **QB** was utilized for real-time monitoring of NADH levels in an Alzheimer's Disease cellular model. PC-12 cells were exposed to oxidative stress induced by varying concentrations of Cu^{2+} (1 mM, 5 mM, 8 mM) for 30 minutes. Subsequently, they were incubated with a 10 µM probe for an additional 30 minutes. To deepen our understanding of NADH changes in Alzheimer's disease, cells treated with 8 mM Cu^{2+} for 30 minutes were further exposed to 10 mM UA for an additional 30 minutes, followed by incubation with probe (10 µM). Fluorescence images were acquired using a confocal microscope (FV 3000, Olympus, Japan) with excitation set at 640 nm and emission collected between 650 and 750 nm.
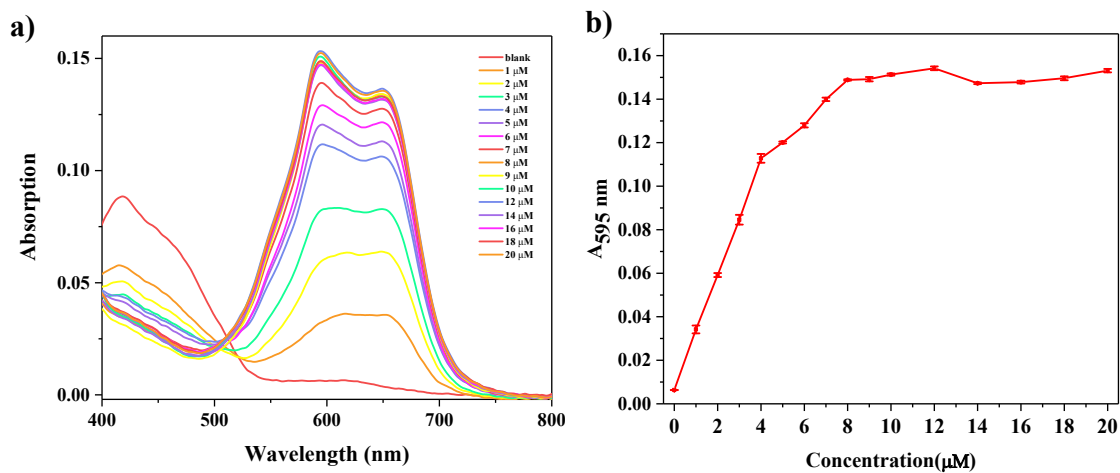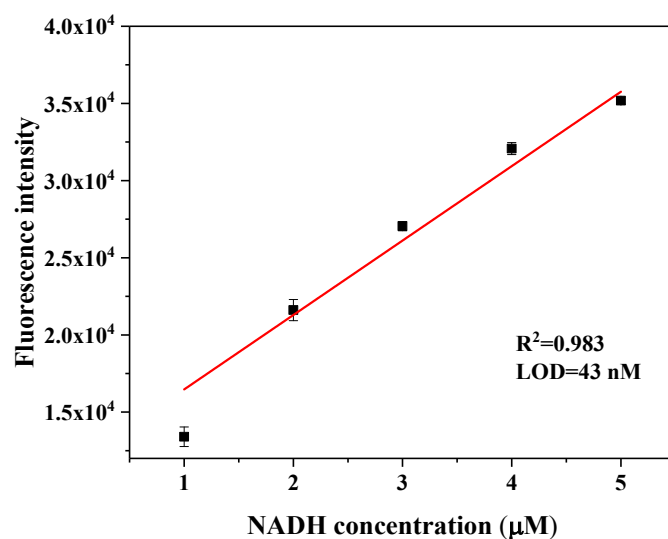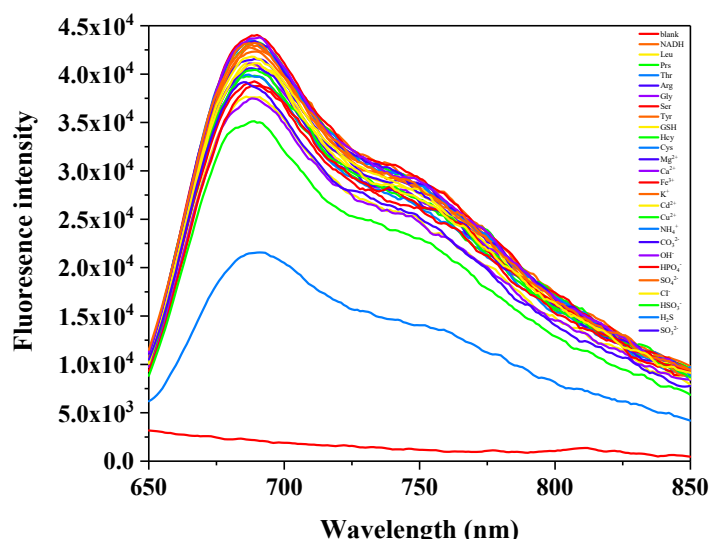
Fig S1. (a) Absorption of probe **QB** (10 µM) with addition of NADH (0-20 µM) in PBS buffer (20 mM, pH 7.4, 0.5% DMSO); (b) The absorption values of the probe at 595 nm with addition of NADH.
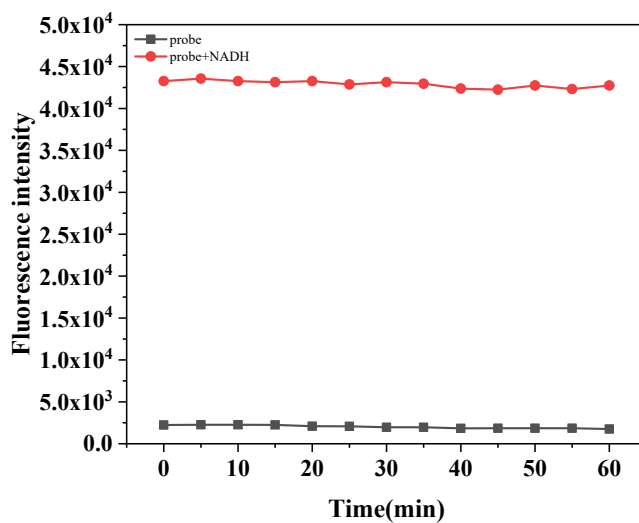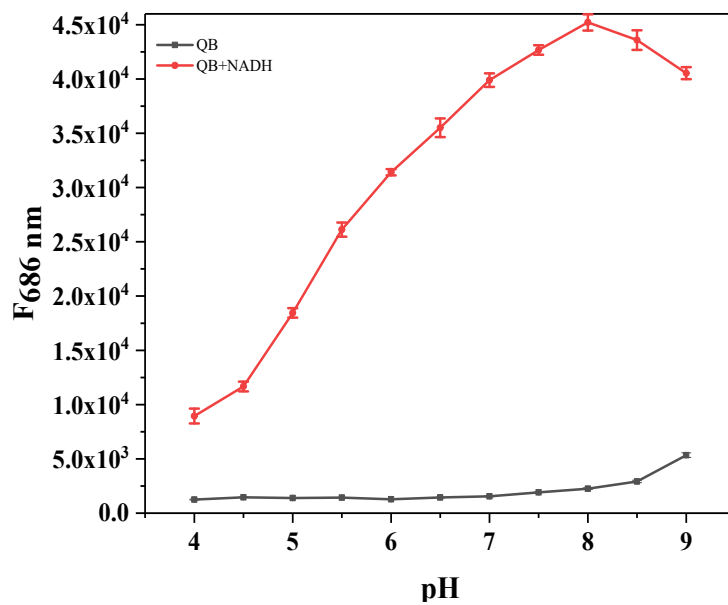

Fig S2. Photostability of 10 µM probe **QB** in the absence or presence of NADH (10 µM).
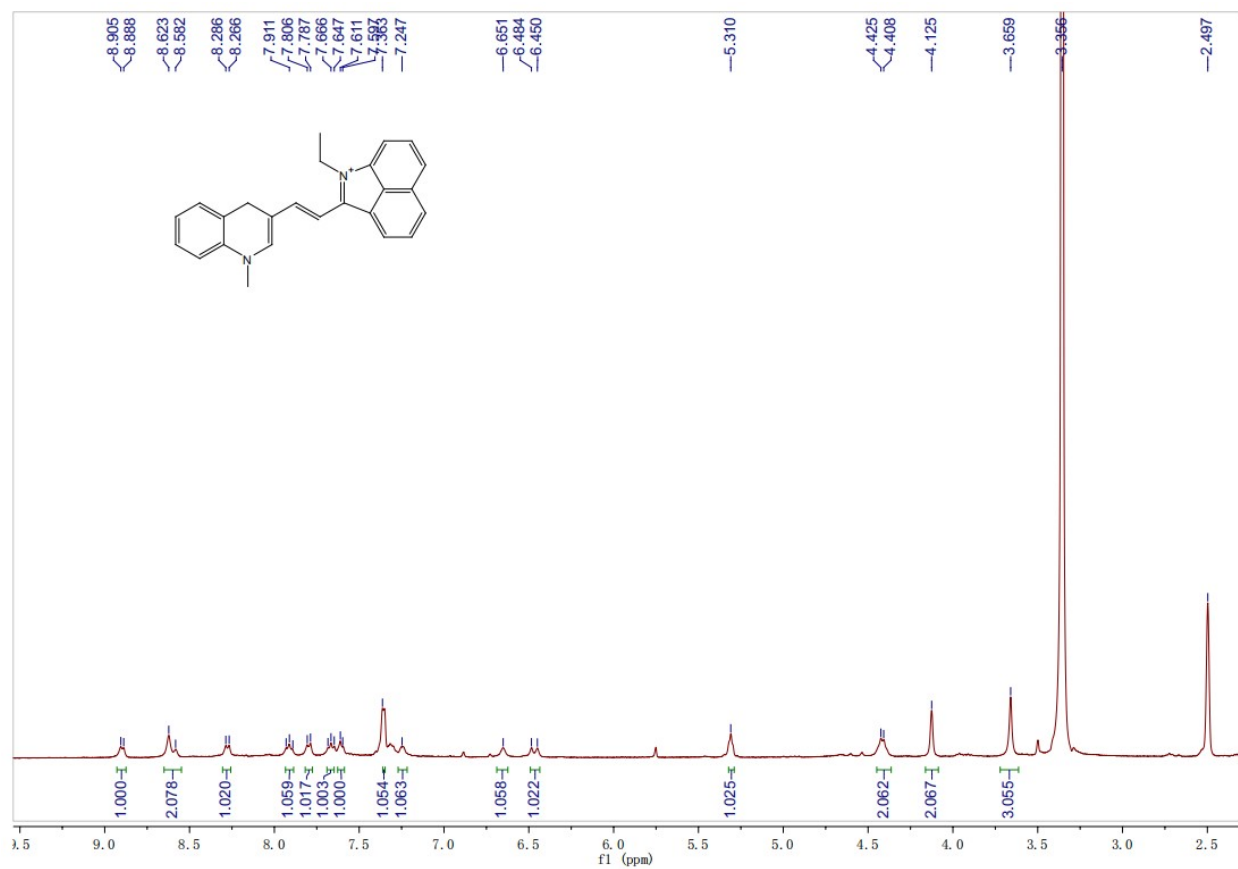
Fig S3. Linear relationship of the flurosecnet intensity at 686 nm ($I_{686\ nm}$) of probe **QB** toward NADH concentration (1−5 μM).

Fig S4. The fluorescence spectrum of probe **QB** (10 μM) towards various analytes(100 μM) in PBS (20 mM, PH 7.4, v/v).

Fig S5. The fluorescence intensity at 686 nm (I_{686nm}) of probe **QB** (10 μM) in the absence (■) or presence (●) of NADH (100 μM) at various pH values.

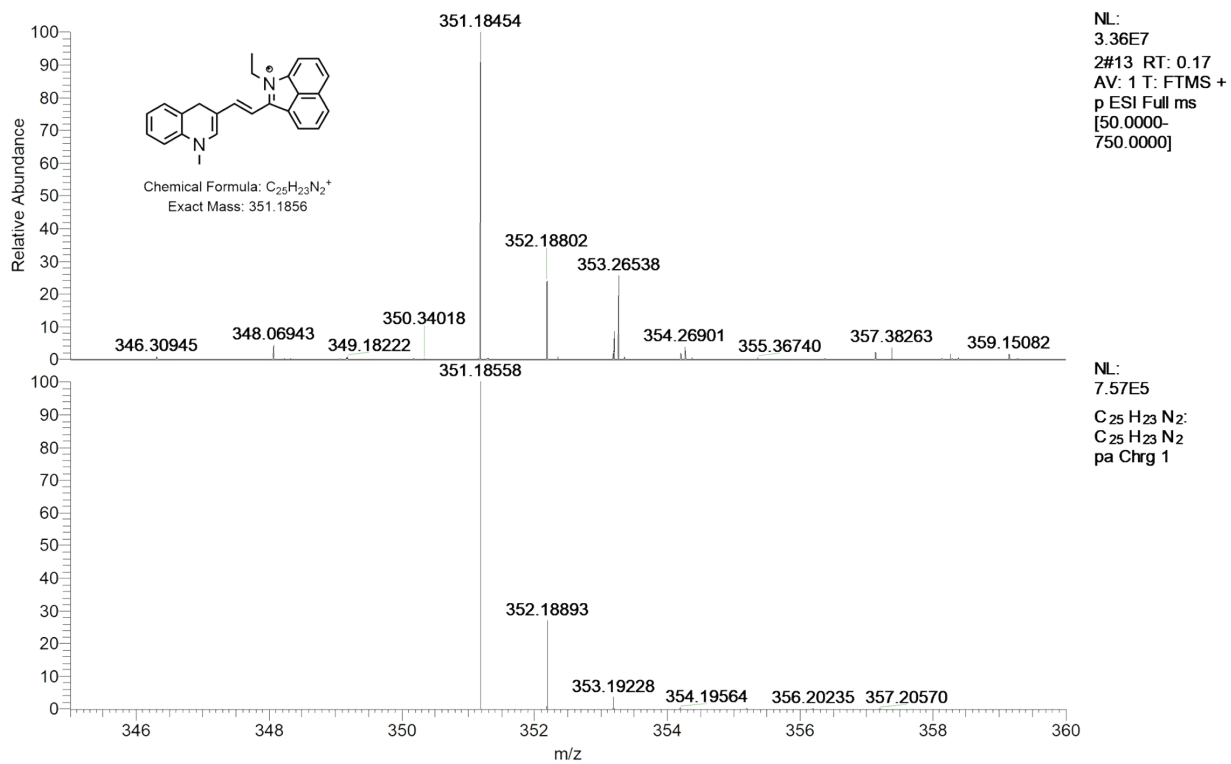**Fig S6.** ^{1}H NMR spectra (400 MHz) of reaction product of probe **QB** with NADH in DMSO-d_6 solution.

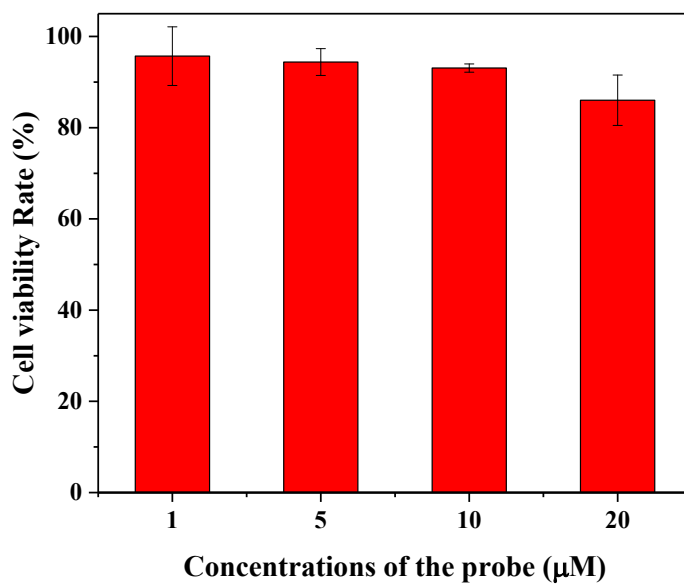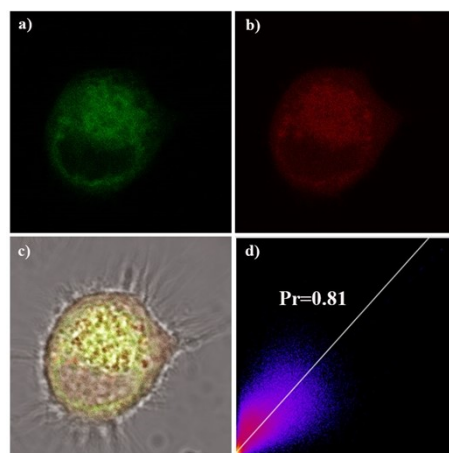**Fig S7.** ESI mass spectrum of reaction product of probe **QB** with NADH.

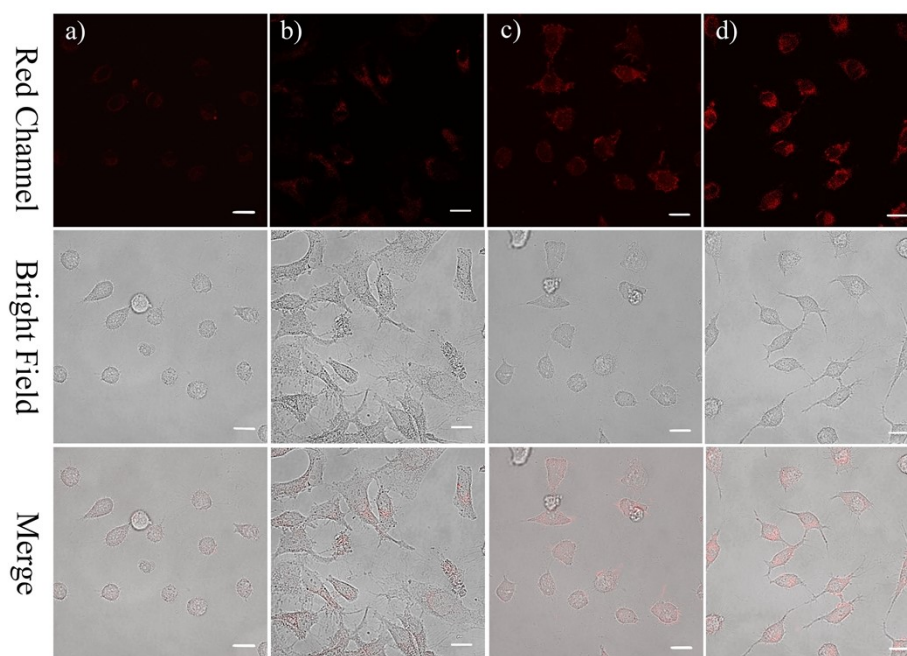**Fig S8.** Viability rate of HeLa cells (%) treated with the probe **QB** (0-20 μM) at 37°C for 24 h.

Fig S9. Confocal fluorescence images of probe **QB** (10 µM) and Mito-Tracker Green (0.12 µM) in Hela cells. (a) green channel, λ_{ex}=488 nm, λ_{em}=500-540 nm. (b) red channel, λ_{ex}=640 nm, λ_{em}= 650-750 nm. (c) the merge of (a) and (b). (d) The person correlation coefficient is 0.81.

Fig S10. Confocal fluorescence images of HeLa cells treated with probe QB. (a) HeLa cells were incubated with 10 µM probe QB for 30 minutes as the control. (b) Pre-treated with 10 µM probe QB, HeLa cells were subsequently incubated with 10 µM NADH, (c) 20 µM NADH, and (d) 50 µM NADH. Scale bar: 20 µm.
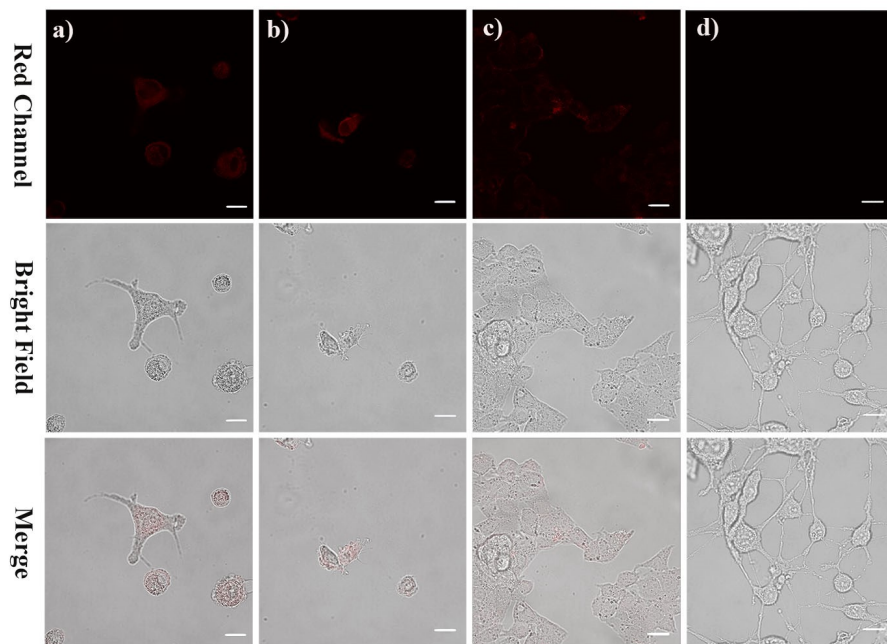
Fig S11. Fluorescence images of 3 types of cancer cells (a: HeLa, b.: A549, c: HepG2) and normal cells (d: 3T3) treated for 30 min with probe QB (10 μM).
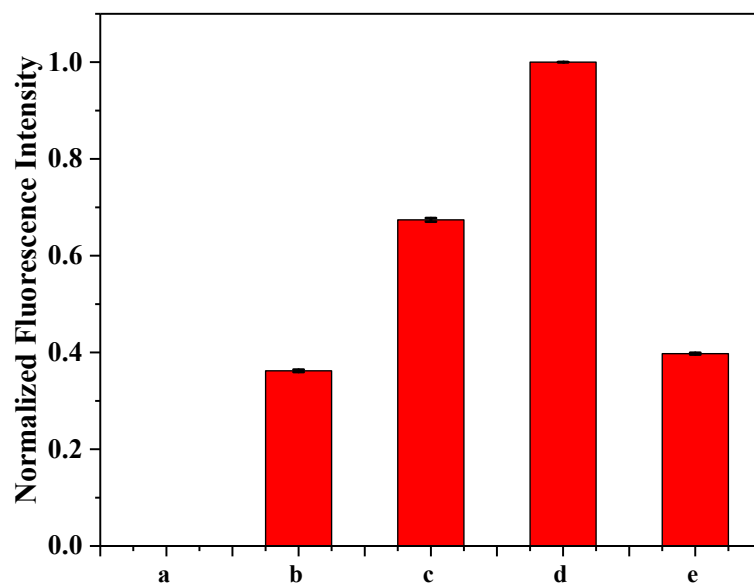
Fig S12. Normalized fluorescence intensity in figure a-e. λ_{ex}=640 nm, λ_{em}= 650-750 nm, scale bar: 20 μm.

NMR and HRMS spectrums of compound **2** and probe **QB**

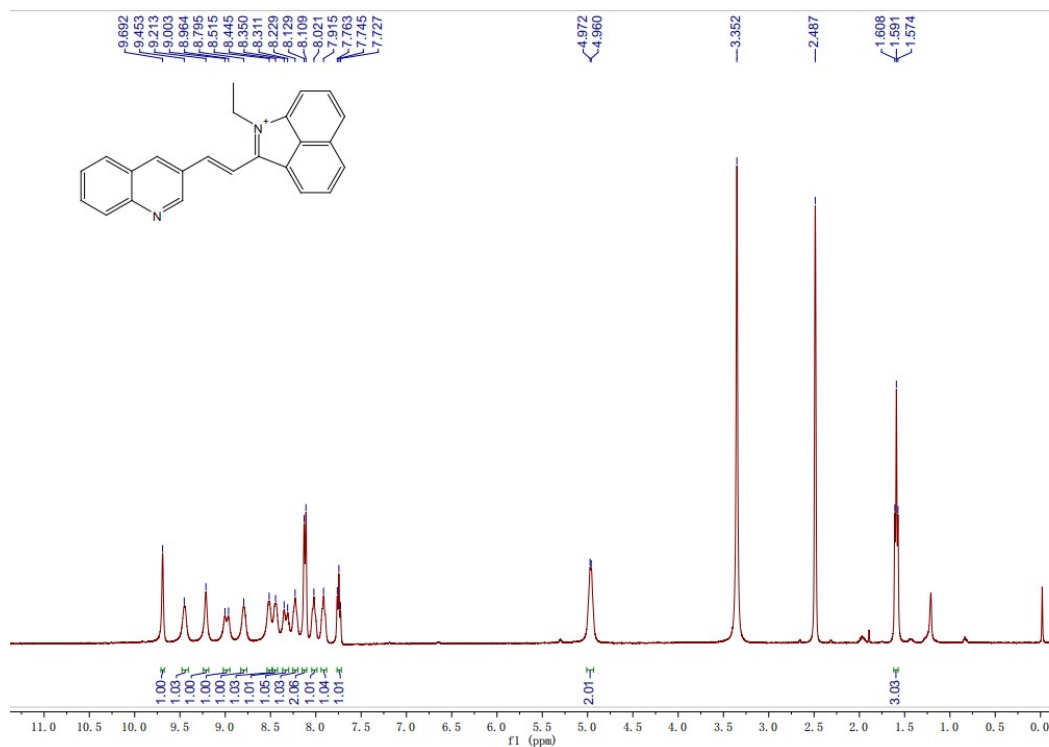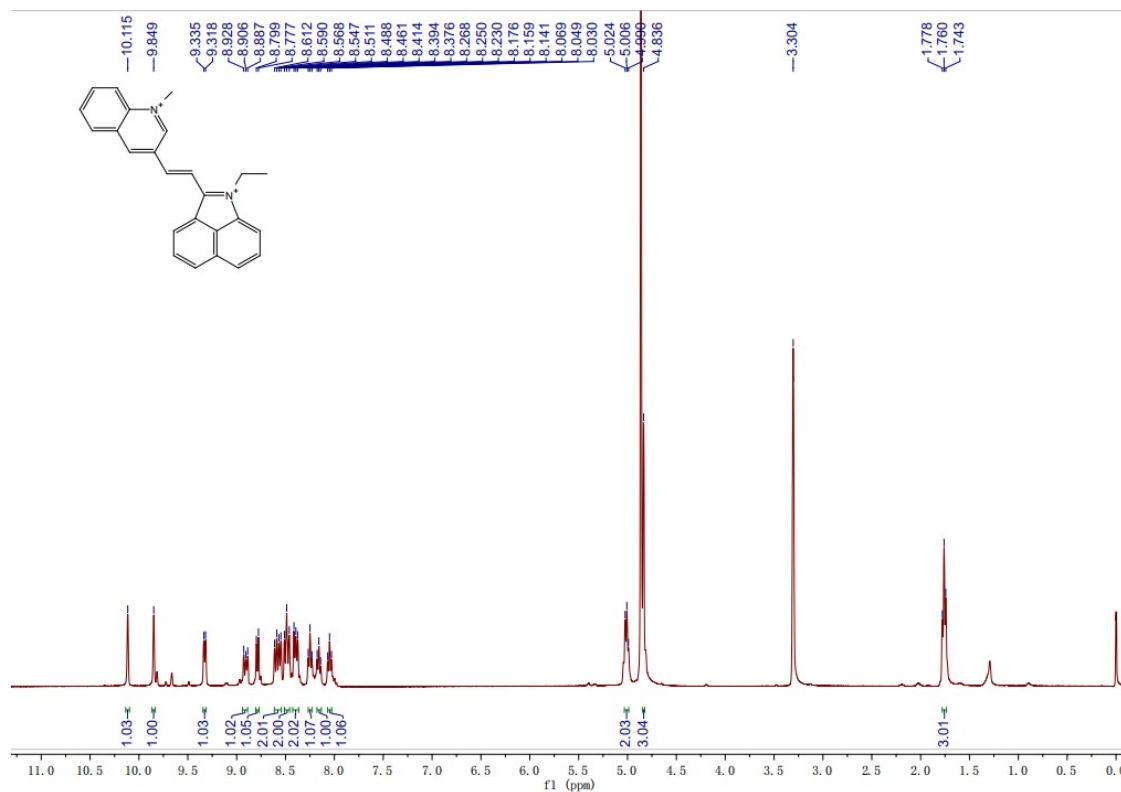**Fig S13.** ^{1}H NMR spectra (400 MHz) of the Compound **2** in DMSO-d$_6$ solution.

Fig S14. ^{1}H NMR spectra (400 MHz) of probe **QB** in CD$_3$OD.
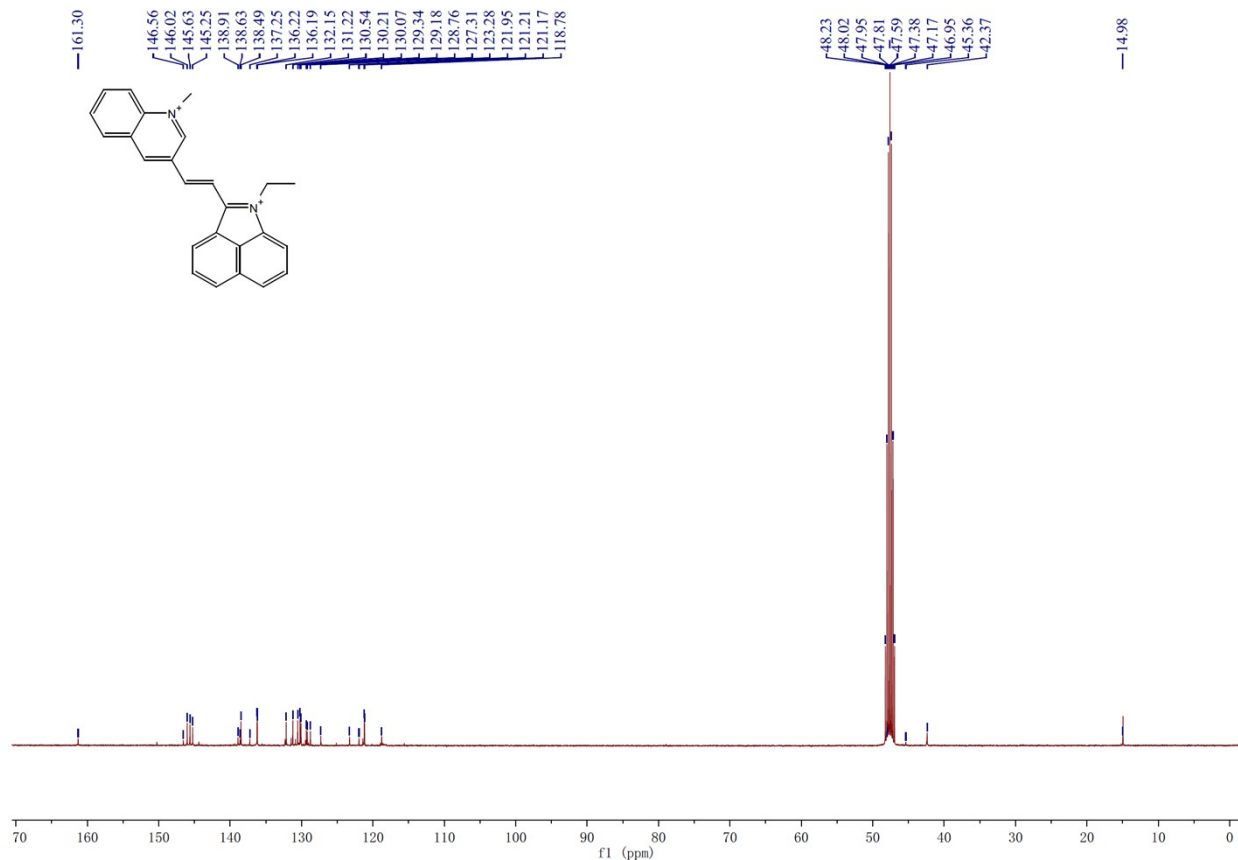
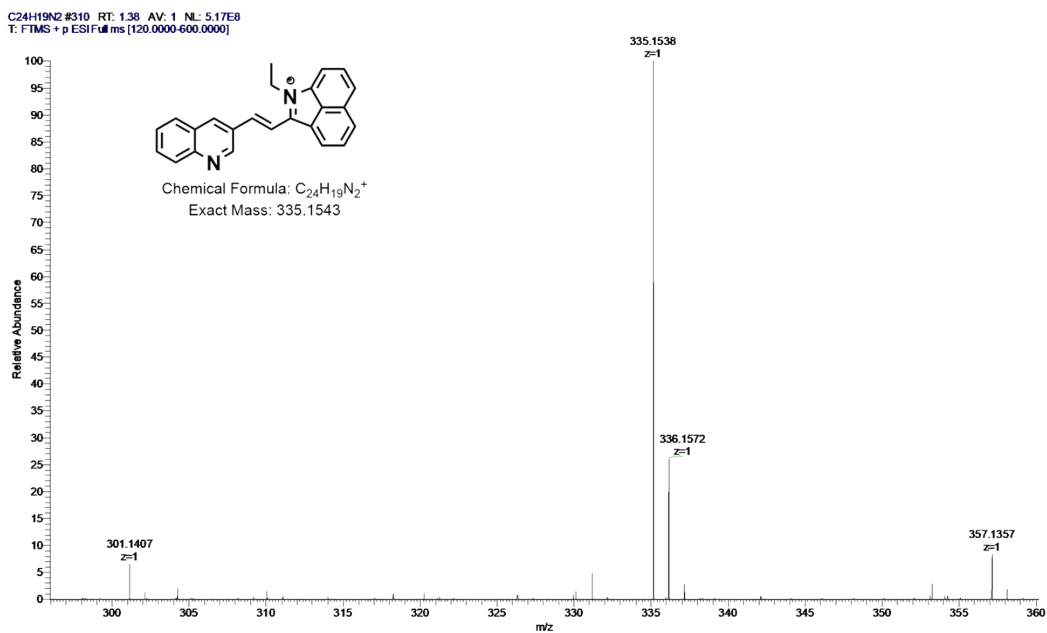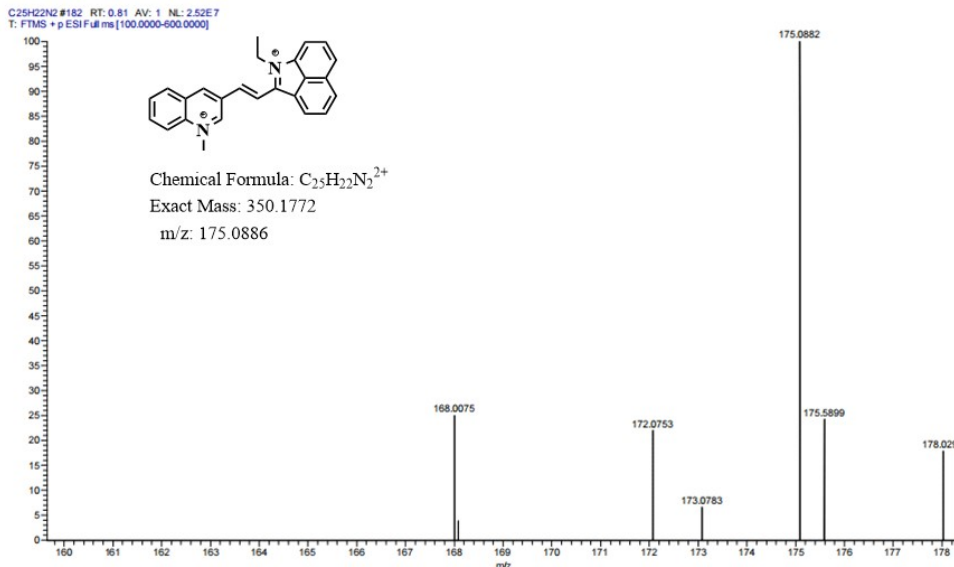**Fig S15.** ^{13}C NMR spectra (100 MHz) of probe **QB** in CD$_3$OD.

Fig S16. ESI mass spectrum of compound **3**.

Fig S17. ESI mass spectrum of probe **QB**.

Reference

(1) Q. Wang, Y. Z. Zhu, D. B. Chen, J. L. Ou, M. Chen, Y. Feng, W. B. Wang, X. M. Meng, *Talanta,* 2023, **257**, 124393.

(2) H. Chang, X. Hu, X. M. Tang, S. W. Tian, Y. D. Li, X. Lv, L. Q. Shang, *Acs Sens*, 2023, **8**, 829-838

(3) M. A. Fomin, R. I. Dmitriev, J. Jenkins, D. B. Papkovsky, D. Heindl, B. König, *Acs Sens*, 2016, **1**, 702-709.

(4) F. Dai, S. X. Zhang, B. Zhou, D. C. Duan, J. R. Liu, Y. L. Zheng, H. Chen, X. Y. Zhang, Y. Zhang, *Anal. Chem.*, 2023, **95**, 1335-1342.

(5) H. Wei, Y. F. Yu, G. H. Wu, Y. Q. Wang, S. Y. Duan, J. Y. Han, W. Y. Cheng, C. Li, X. Tian, X. J. Zhang, *Sens. Actuators B Chem.*, 2022, **350**, 130862.

(6) M. Z. Li, C. Liu, W. J. Zhang, L. F. Xu, M. M. Yang, Z. L. Chen, X. X. Wang, L. L. Pu, W. L. Liu, X. S. Zeng, T. H. Wang, *J Mater Chem B.* 2021, **9**, 9547-9552.

(7) Y. H. Zhao, K. Y. Wei, F. P. Kong, X. N. Gao, K. H. Xu, B. Tang, *Anal. Chem.*, 2019, **91**, 1368-1374.

(8) X. H. Pan, Y. H. Zhao, T. T. Cheng, A. S. Zheng, A. B. Ge, L. X. Zang, K. H. Xu, B. Tang, *Chem. Sci.*, 2019, **10**, 8179-8186.

(9) A. Podder, V. P. Murali, S. Deepika, A. Dhamija, S. Biswas, K. K. Maiti, S. Bhuniya, *Anal. Chem.* 2020, **92**, 12356-12362.

(10) A. Podder, S. Koo, J. Lee, S. Mun, S. Khatun, H. G. Kang, S. Bhuniya, J. S. Kim, *Chem. Commun.* 2019, **55**, 537-540.

(11) 14 J. H. Joo, M. Won, S. Y. Park, K. Park, D. S. Shin, J. S. Kim, M. H. Lee, *Sens. Actuators B Chem.*, 2020, **320**, 128360.

(12) D. L. Arachchige, S. K. Dwivedi, S. Jaeger, A. M. Olowolagba, M. Mahmoud, D. R. Tucker, D. R. Fritz, T. Werner, M. Tanasova, R. L. Luck, H. Liu, *ACS Appl. Bio Mater.,* 2023, **6**, 3199-3212.

(13) D. L. Arachchige, S. K. Dwivedi, M. Waters, S. Jaeger, J. Peters, D. R. Tucker, M. Geborkoff, T. Werner, R. L. Luck, B. Godugu, H. Liu, *J. Mater. Chem. B.* 2024, **12**, 448-465.

(14) S. K. Dwivedi, D. L. Arachchige, M. Waters, S. Jaeger, M. Mahmoud, A. M. Olowolagba, D. R. Tucker, M. R. Geborkoff, T. Werner, R. L. Luck, B. Godugu, H. Liu, *Sens. Actuators B Chem.*, 2024, **402**, 135073.

(15) K. Q. Ma, H. Yang, X. K. Wu, F. J. Huo, F. Q. Cheng, C. X. Yin, *Angew. Chem. Int. Ed.*, 2023, **62**, e202301518.

(16) L. Guan, H. Sun, J. Xiong, W. Hu, M. Ding, Q. Liang, *Sens. Actuators B Chem.*, 2022, **373**, 132694.

(17) L. Yuan, W. Y. Lin, Y. T. Yang, H. Chen, *J. Am. Chem. Soc.*, 2012, **134**, 1200-1211